

Self-generated magnetic fields associated with a laser-produced plasma

L. L. McKee, * R. S. Bird, and F. Schwirzke

Naval Postgraduate School, Monterey, California 93940

(Received 16 July 1973)

The dependence of the self-generated magnetic fields associated with a laser-produced plasma on position, time, incident laser power, and nitrogen background pressure has been investigated. The presence of the ambient background is found to influence the generation of the fields during the laser irradiation of the plasma. This influence continues long after laser shutoff and causes the fields to reverse their direction.

I. INTRODUCTION

It has generally been assumed that unless an external magnetic field is applied, a laser-produced plasma (or laser plasma) is expanding under essentially field-free conditions. However, it has been discovered that a magnetic field may spontaneously arise when a laser plasma is produced by the laser-induced breakdown of a gas¹ or by the laser irradiation of a solid target.² From these and subsequent investigations³⁻⁶ it appears that self-generated magnetic fields may arise under very general conditions during the production of a laser plasma. In fact, these fields appear to be an inherent property of laser plasmas, and recent results of computer calculations^{7,8} have demonstrated the importance of including the generation of these fields in theoretical treatments of laser plasmas.

This article describes a detailed study of the self-generated magnetic fields associated with a laser plasma. The results of the experimental study are discussed in terms of a thermal source term for magnetic fields.

II. EXPERIMENTAL APPARATUS

The neodymium-doped-glass laser system used consisted of a Q -switched oscillator stage and a single amplifier stage. The output of the laser system ranged from about 4 J to about 11.5 J in a 25-nsec pulse or about 150–450 MW.

The target was a 0.005-in-thick Mylar ($C_{10}H_8O_4$) foil. The laser beam struck it at an angle of 30° to the flat-target's normal and burned a 2-mm-diameter hole in the target on each shot. Since the resulting laser plasma streams out normal to the target's surface regardless of the angle of incidence of the laser beam,⁹ this choice of angle allowed the laser plasma to be probed along its flow direction without having the laser beam strike the probe.

The target was located in a vacuum chamber into which nitrogen gas could be admitted to provide an ambient background for the expanding laser plasma. The nitrogen gas pressures used varied from 10^{-4} to 1 Torr.

The self-generated magnetic fields were detected by means of a small (~ 1 -mm-diameter coil) inductive magnetic probe. The probe signal, which was proportional to dB/dt , was conducted via 50- Ω cable to the input of an oscilloscope, where the signal was integrated by means of a passive RC integrator before being displayed. The probe signals were sufficiently free of electrostatic noise pickup to allow field signals as low as 1 G in magnitude to be resolved. A field of this magnitude gave about a 0.2-mV integrated probe signal and the oscilloscope had a maximum vertical sensitivity of 1 mV/cm.

III. EXPERIMENTAL RESULTS

The target normal forms the z axis for a convenient cylindrical coordinate system to reference the probe positions. The origin is the point at which the laser strikes the target, and the $+z$ direction is the direction in which the resultant laser plasma expands. The self-generated magnetic fields were found to be mainly in the azimuthal direction about the z axis and pointed in the $-\theta$ direction (as if caused by a conventional current in the $-z$ direction). This is in basic agreement with the results of Stamper *et al.*²

The magnetic-field signals detected at fixed positions were basically pulse shaped with relatively fast rises and relatively slower decays, as shown in Fig. 3 of Ref. 6. As the magnetic probe was moved away from the target, in general the probe signals were delayed further in time, and their durations increased.

The most striking result of this investigation was the strong dependence of the self-generated magnetic fields on the ambient pressure of the nitro-

gen background gas.^{3,4,6} Figure 1 shows the variation of the maximum azimuthal magnetic field at a fixed position (i.e., the peak field in the probe signal) with the pressure of the nitrogen background gas.

There are three regions evident in Fig. 1. For pressures lower than 1 mTorr, the magnitude of the magnetic field does not depend on the nitrogen gas pressure. For pressures in the range of 1–200 mTorr, the magnitude of the field rises very sharply with increasing pressure. At pressures higher than 200 mTorr, the magnitude of the field rapidly decreases with increasing pressure. This curve exhibits an amplification of the field magnitude by a factor of 6 as the ambient gas pressure was increased from 1 to 200 mTorr.

The dependences of the self-generated magnetic fields on background gas pressure and on incident laser power are combined in Fig. 2. The curve for each laser power in this figure has the same basic shape. Thus, for these ranges of laser powers and ambient pressures, the laser power served only to scale the magnetic fields. The ambient gas pressure was the more fundamental parameter. All further field measurements were taken for a fixed incident laser power of 300 MW.

The symmetry of the azimuthal magnetic fields about the z axis was tested. Within the experimental error of 10%, the magnitude of the azimuthal field was found to be the same when the field was measured at different angular positions along several circles centered on, and normal to,

the z axis. Hence, the azimuthal magnetic fields were axisymmetric about the z axis.

The azimuthal magnetic fields were mapped extensively in the $\theta = 0^\circ$ plane (vertical plane above the z axis) for three ambient pressures of nitrogen: 0.1, 5, and 250 mTorr. They represent, respectively, pressures corresponding to the pressure-independent region, the onset of the field amplification region, and the field "damping" region in Fig. 1. The results of the two-dimensional mapping are presented as contour plots of the magnitude of the field. Figure 3 shows the contour plots of the maximum azimuthal fields measured at each point in the plane for any time.

In these plots, the foil target is located at the left edge of the plots and is perpendicular to the plane of the figure. The laser beam comes in from the right at 30° to the plane of the figure and strikes the target at the lower-left corner of the plots. The resulting laser plasma then expands to the right. The region where the laser beam intersects the plane of the figure cannot be probed due to interference with the laser beam and is left blank. The direction of the field is perpendicular to the plane of the contour plots. A positive field value corresponds to an orientation of the field in the $-\theta$ direction about the z axis and a negative value to the opposite azimuthal orientation. Because of the symmetry of the azimuthal fields, these contour plots give full three-dimensional representations of the field when they are

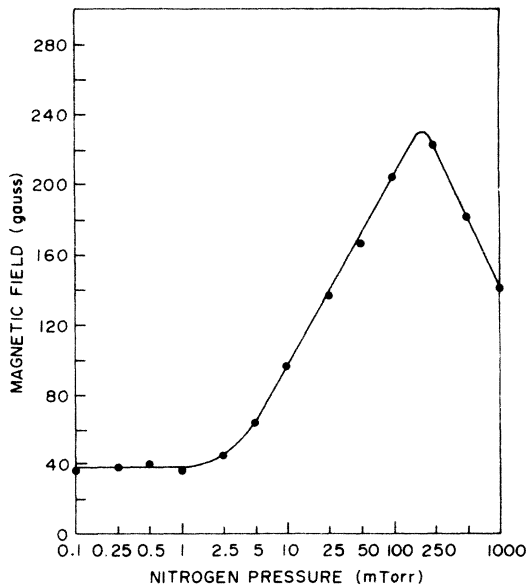


FIG. 1. Maximum B_θ at $z = 4$ mm, $r = 3$ mm vs nitrogen background pressure for an incident laser power of 300 MW.

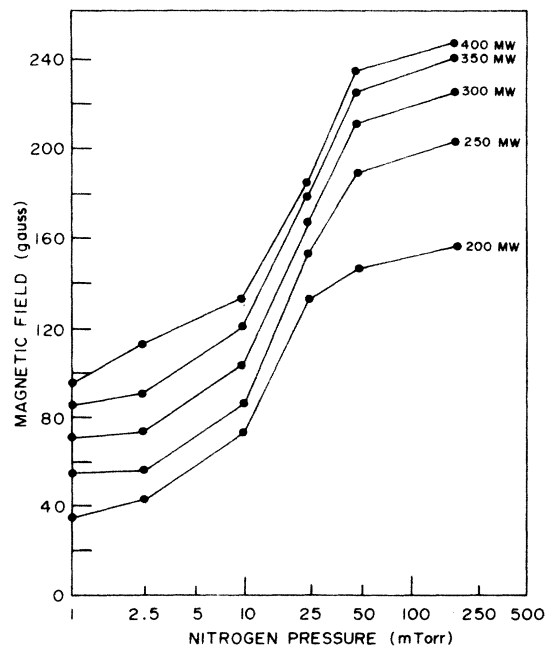


FIG. 2. Maximum B_θ at $z = 4$ mm, $r = 3$ mm vs nitrogen background pressure for a given laser power.

rotated about the z axis.

Figure 3 illustrates the decrease of the magnitude of the magnetic fields with distance. For each pressure, the magnitude of the fields decreased more sharply in the radial direction than in the axial direction. Also, Fig. 3 shows that the magnetic field decreased more rapidly with distance for an ambient nitrogen pressure of 250 mTorr than for the other two pressures.

The manner in which the magnetic fields decayed with time along the $r = 4$ mm line is shown in Fig. 4. This figure gives the largest field measured at any axial position along $r = 4$ mm at each instant of time. The reference time ($t = 0$) for the time studies was the time at which the laser power attained its maximum value. Figure 4 shows that the field in the 250-mTorr case decayed significantly more rapidly with time than did the fields in the other two pressure cases.

The results of mapping the magnetic fields in the $\theta = 0^\circ$ plane for the three ambient pressures of nitrogen were time-resolved. The contour plots derived from these measurements showed that the magnetic-field contours, like the laser plasma, expanded and propagated out from the target. The

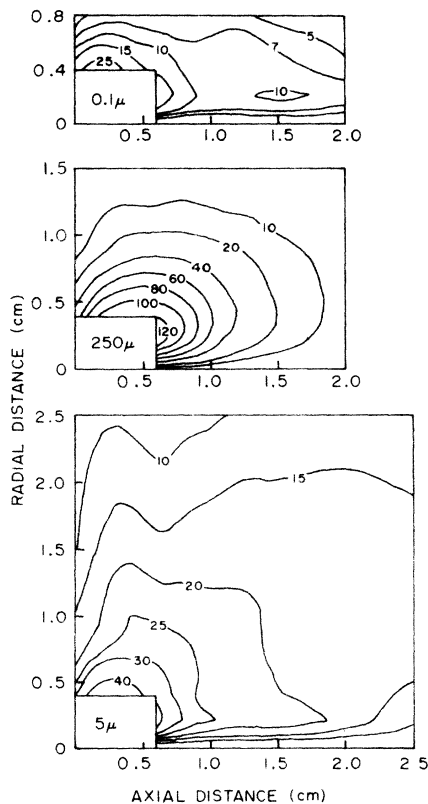


FIG. 3. Maximum B_θ for various pressures of nitrogen background gas.

propagation velocity of the position of highest field was about 10^7 cm/sec for ambient pressures of 0.1 and 5 mTorr of nitrogen and about 6.5×10^6 cm/sec for 250 mTorr.

Figures 5(a)–5(c) illustrate the expansion and flow of the magnetic field contours out from the target. Even at the peak of the laser pulse, Fig. 5(a) shows that there were differences in the magnitudes of the fields for the three ambient-pressure cases. The largest observed fields did not appear until 40 nsec [Fig. 5(b)], since the largest field contours had to flow out of the inaccessible region in order to be observed. Apparently much larger fields occurred at earlier times close to the target, but these large fields decayed sharply as they flowed out of the inaccessible region, as Fig. 4 implies. As the expansion and flow of the field contours progressed, distinctions between the shapes and spatial extents of the contours for the three ambient pressure cases became apparent, as Fig. 5(c) shows. The chief distinctions at these early times were that the field contours for 0.1 mTorr exhibited a relatively small radial expansion and the contours for 5 mTorr had the broadest spatial extent.

Figures 6(a) and 6(b) show the late-time characteristics of the field contours. By 300 nsec, Fig. 6(a) shows that the highest field contours were flowing out of the observation region for 0.1 mTorr and the contours for 5 mTorr had expanded significantly in the radial direction. The contours for 250 mTorr had broken up into several islands at that time, and the field in two of these islands

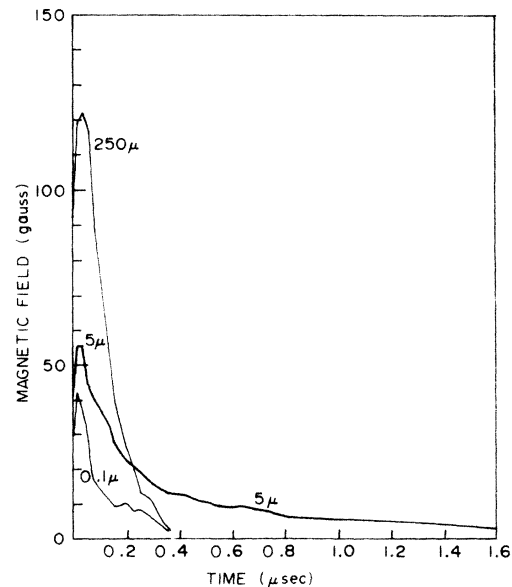


FIG. 4. Maximum B_θ along $r = 4$ mm vs time for various pressures of nitrogen background gas.

had reversed its direction. Figure 6(b) shows that this field reversal continued to develop until the field had reversed its direction everywhere in the observation region for 250 mTorr, and the magnitude of the field increased in the reverse direction. A weaker reversed field also developed for 0.1 mTorr at these late times, as Fig. 6(b) shows.

At times later than 700 nsec, the reversed fields for 0.1 and 250 mTorr decreased in magnitude in the observation region. The field for 5 mTorr of nitrogen finally reversed its direction at about 1.3 μ sec near the target.

The current-density distributions which produced the self-generated magnetic field were determined by applying

$$\nabla \times \vec{B} = \mu_0 \vec{j} \quad (1)$$

to the magnetic field data. The typical current-density pattern for 250 mTorr is displayed in Fig. 7. The current flow was toroidal in three dimensions with no current flow in the azimuthal direction. The largest current densities deduced for the three pressures were 360 A/cm² for 0.1 mTorr, 557 A/cm² for 5 mTorr, and 1.53×10^3 A/cm² for 250 mTorr of nitrogen.

IV. DISCUSSION

The equation which governs the self-generated magnetic fields is⁶

$$\frac{\partial \vec{B}}{\partial t} = \nabla \times (\vec{v}_e \times \vec{B}) + \frac{1}{\mu_0 \sigma} \nabla^2 \vec{B} + \frac{k}{en_e} \nabla T_e \times \nabla n_e, \quad (2)$$

where v_e , n_e , and T_e are the electron flow velocity, density, and temperature, respectively, and σ is the scalar electrical conductivity. The three terms on the right-hand side of Eq. (2) describe the convection, diffusion, and generation of magnetic field, respectively.

According to the source term in Eq. (2)

$$\vec{S} = \frac{k}{en_e} \nabla T_e \times \nabla n_e, \quad (3)$$

the geometry of the magnetic field is determined by the geometry of the laser plasma. A laser plasma produced from a planar target is ideally axisymmetric about its expansion direction so that there are no azimuthal density or temperature gradients. Then according to Eq. (3), the field will be generated entirely in the azimuthal direction and will be symmetric about the z axis, as

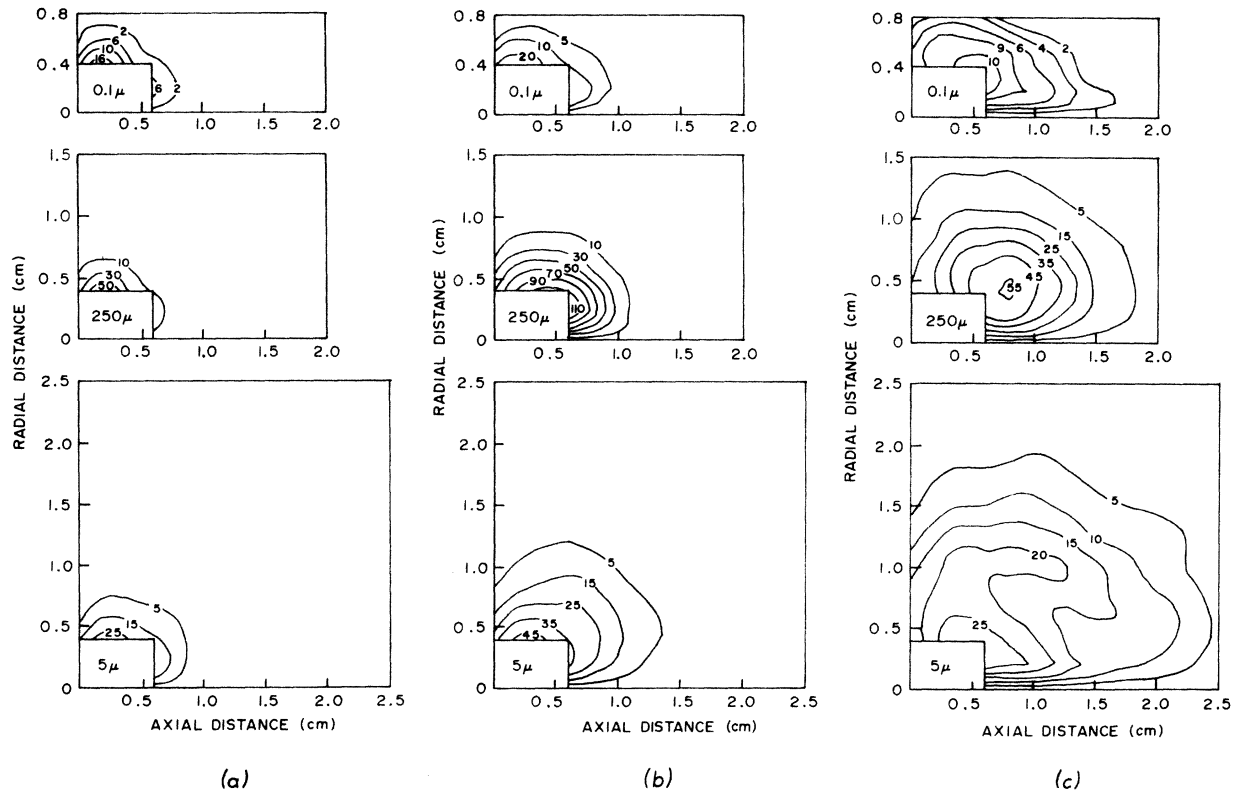


FIG. 5. B_θ at (a) 0 nsec, (b) 40 nsec, (c) 120 nsec for various pressures of nitrogen background gas.

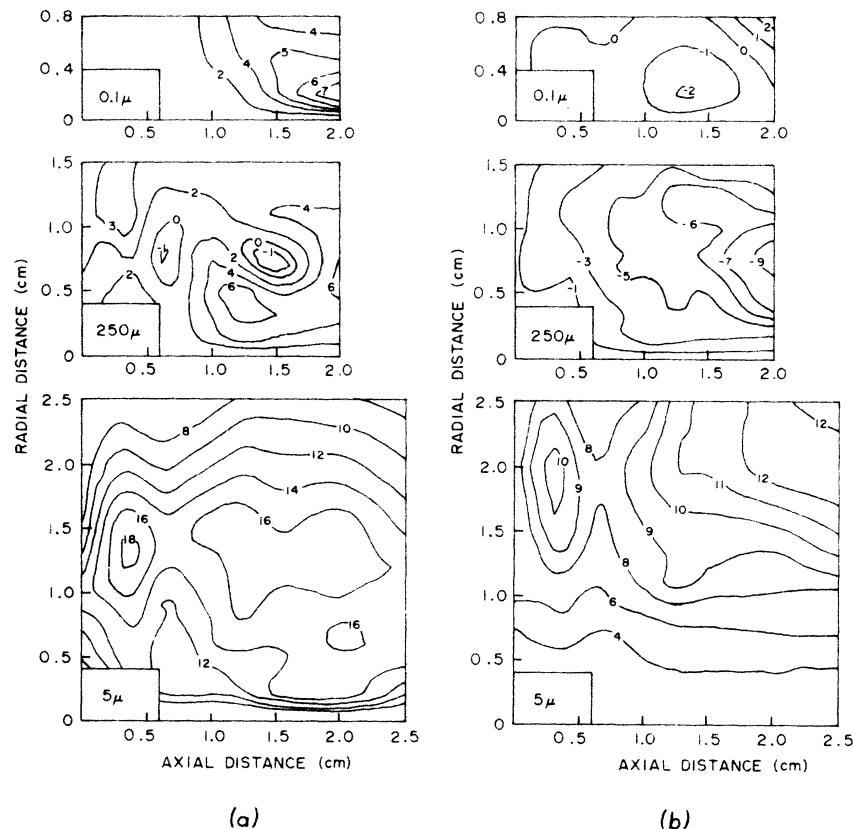


FIG. 6. B_θ at (a) 300 nsec, (b) 700 nsec for various pressures of nitrogen background gas.

observed.

The source term also shows that no field generation will occur unless ∇T_e and ∇n_e are nonparallel. A computer study has shown that during the laser heating of the plasma, the largest contribution to the source term comes from a temperature gradient in the $-r$ direction and the density gradient in the $-z$ direction.¹⁰ The temperature gradient is a consequence of the finite radial extent of the laser beam and arises near the radial edge of the laser-heated region of the plasma. This combination of ∇T_e and ∇n_e will generate magnetic field in the $-\theta$ direction, as observed initially.

The strongest field production can be expected to occur at the front of the expanding laser plasma, since the quantity $(1/n_e)\nabla n_e$ in Eq. (3) is largest there.⁵ Since this is also the region where the laser plasma and the ambient background will interact, it is possible for the background to influence the generation of the fields. The ambient gas is photoionized by energetic photons from the laser plasma. A strong momentum coupling between the resulting ambient plasma and the streaming laser plasma has been observed, even during the laser irradiation of the laser plasma.^{11, 12} This momentum transfer causes deceleration of the laser plasma at its front, resulting

in an increase of the density gradient there due to plasma pileup. The observation that the rate of momentum transfer increases with ambient pressure,^{11, 12} implies that the density gradient at the front of the laser plasma increases with ambient pressure. Consequently, Eq. (3) shows that the rate at which the magnetic field is generated in

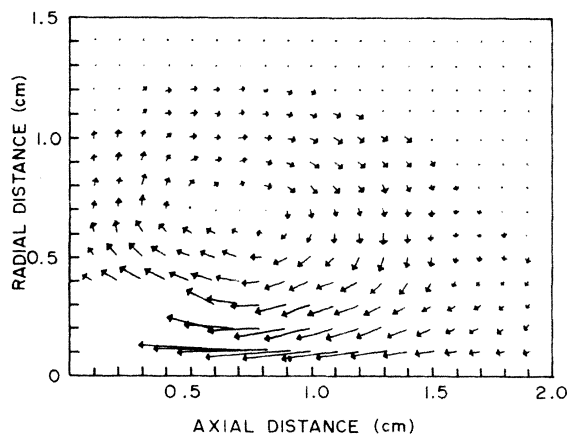


FIG. 7. Current density at 120 nsec for 250 mTorr of nitrogen background gas. The magnitude of the largest current density at this time is 612 A/cm².

the front region increases with ambient pressure. As a result, larger fields are generated at higher pressures, as Fig. 1 shows (for pressures less than 200 mTorr).

In order to show that the observed increase of the field strength with ambient pressure was due to enhanced field generation and not to enhancement of the convection term in Eq. (2) (via field compression), the total magnetic flux was calculated for the different ambient pressures. Since the convection term conserves flux, any increase of the flux will be due to an increase of the source term. The maximum observed fluxes, as calculated from the contour plots, were 5.8 G cm² for 0.1 mTorr and 46.4 G cm² for 250 mTorr. Then the flux increases by a factor of 8, while Fig. 1 shows that the field was amplified by a factor of about 6 at 250 mTorr. Hence the increase in field strength with pressure can be accounted for entirely by enhanced field generation.

The largest fields are generated during the laser heating of the plasma. However, field generation can continue after laser shutoff. In fact, the appearance of the reversed field at later times [Figs. 6(a) and 6(b)] is evidence that field generation was occurring at those times. Examination of Eq. (2) reveals that the reversal of an axisymmetric field can only occur via the source term. Field must be generated in the reverse direction. Further, it was observed that the reversed field was larger and occurred earlier as the pressure was increased above 250 mTorr, indicating that the reversed source term, like the initial source term, increased with ambient pressure.

The source term is apparently reversed as a consequence of the interaction between the laser plasma and the ambient plasma. After laser shutoff the temperature gradient in the $-r$ direction decreases due to heat conduction. However, as the two plasmas interact, the laser plasma is heated at its front. This heating process will produce an axial temperature gradient which is in the $-z$ direction at the very front of the laser plasma. Since there is a density gradient in the $-r$ direction in this region, a reversed source term will arise at the front, as Eq. (3) shows. Because the two plasmas interact more strongly at higher pressures, this reversed source term will increase with ambient pressure.

The reversal of the source term at the front of the expanding laser plasma explains the rapid decay rate of the field observed for 250 mTorr in Fig. 4. When the source term reverses, it first acts to reduce the magnitude of the field generated

initially. Since the reversed source term increases with ambient pressure, the rate of decrease of the original field also increases with ambient pressure, as Fig. 4 shows. The decrease of the field strength with pressure for pressures above 200 mTorr in Fig. 1 resulted when the field for higher ambient pressures decreased in magnitude at a higher rate as it was being carried by the expanding laser plasma to that probe position.

It should be noted here that an increase of the diffusion term in Eq. (2) with ambient pressure would not adequately account for the higher rate of decrease of the field at higher pressures. The diffusion term cannot cause the field reversal associated with the rapid decay rates.

Reversed field should also be generated behind the front region. The coupling between the two plasmas causes plasma density to pileup at the front, so that behind the front there will be a density gradient in the $+r$ direction. In addition, the heating at the front due to the interaction produces a temperature gradient in the $+z$ direction behind the front. These gradients will combine to generate reversed field. Hence, two regions of field reversal can be expected to result from the coupling between the two plasmas.

Examination of Figs. 6(a) and 6(b) indicates that the field reversal there was occurring in the region behind the front, where the density gradient was in the $+r$ direction. Apparently, the field reversal at the front occurred outside of the mapping region.

V. CONCLUSION

On the basis of the results presented here and previous results,^{4,6} it appears that the presence of an ambient gas can significantly influence the generation of the self-generated magnetic fields. This influence begins during the laser irradiation of the plasma and continues long after laser shutoff. The fact that fields can be generated in the absence of laser radiation is a consequence of the thermal nature of the source term in Eq. (2). However, a more detailed comparison between the data and the proposed theory will require density and temperature gradient measurements.

ACKNOWLEDGMENTS

The authors would like to thank Mr. H. M. Herreman for his valuable assistance in the experimental work. This work was supported by the Air Force Office of Scientific Research under AFOSR Grant No. MIPR-0004-69 and by the Office of Naval Research.

- *Present address: Air Force Weapons Laboratory,
Kirtland AFB, N. M. 87117.
- ¹V. N. Korobkin and R. V. Serov, Zh. Eksp. Teor. Fiz. Pis'ma Red. 4, 103 (1966)[JETP Lett. 4, 147 (1966)].
- ²J. A. Stamper, K. Papadopoulos, R. N. Sudan, S. O. Dean, E. A. McLean and J. M. Dawson, Phys. Rev. Lett. 26, 1012 (1971).
- ³F. Schwirzke and L. L. McKee, in *Proceedings of the Fifth European Conference on Controlled Fusion and Plasma Physics* (Grenoble, France 1972), p. 63.
- ⁴F. Schwirzke and L. L. McKee, Bull. Am. Phys. Soc. 17, 1027 (1972).
- ⁵R. S. Case, Jr., Bull. Am. Phys. Soc. 17, 1026 (1972).
- ⁶R. S. Bird, L. L. McKee, F. Schwirzke, and A. W. Cooper, Phys. Rev. A 7, 1328 (1973).
- ⁷G. B. Zimmerman, E. T. Scharleman, and L. L. Wood, Bull. Am. Phys. Soc. 17 1035 (1972).
- ⁸M. Widner, T. Wright, and J. Freeman, Bull. Am. Phys. Soc. 17, 1047 (1972); and M. Widner and T. Wright (private communication).
- ⁹J. F. Ready, *Effects of High-Power Laser Radiation* (Academic, New York, 1971), p. 165.
- ¹⁰T. P. Wright and M. M. Widner, Bull. Am. Phys. Soc. 17, 1027 (1972).
- ¹¹S. O. Dean, E. A. McLean, J. A. Stamper, and H. R. Griem, Phys. Rev. Lett. 27, 487 (1971).
- ¹²J. L. Bobin, Y. A. Durand, Ph. P. Langer, and G. Tonon, J. Appl. Phys. 39, 4184 (1968).